Ferroelastically and magnetically co-coupled resistive switching in $Nd_{0.5}Sr_{0.5}MnO_3$/PMN-PT(011) multiferroic heterostructures

Ming Zheng,[1,2,a)] Xiao-Ke Xu,[3] Hao Ni,[2,4] Ya-Ping Qi,[2] Xiao-Min Li,[3] and Ju Gao[2,5]
[1]*Department of Applied Physics, The Hong Kong Polytechnic University, Kowloon, Hong Kong*
[2]*Department of Physics, The University of Hong Kong, Pokfulam Road, Hong Kong, Hong Kong*
[3]*State Key Laboratory of High Performance Ceramics and Superfine Microstructure, Shanghai Institute of Ceramics, Chinese Academy of Sciences, Shanghai 200050, China*
[4]*College of Science, China University of Petroleum (East China), Qingdao 255680, China*
[5]*School of Mathematics and Physics, Suzhou University of Science and Technology, Suzhou 215009, China*

(Received 14 November 2017; accepted 6 March 2018; published online 19 March 2018)

The phase separation, i.e., the competition between coexisting multi-phases, can be adjusted by external stimuli, such as magnetic field, electric field, current, light, and strain. Here, a multiferroic heterostructure composed of a charge-ordered $Nd_{0.5}Sr_{0.5}MnO_3$ thin film and a ferroelectric $Pb(Mg_{1/3}Nb_{2/3})O_3$-$PbTiO_3$ single crystal is fabricated to investigate the lattice strain and magnetic field co-control of phase separation in resistive switching. The stable and nonvolatile resistance tuning is realized at room temperature using the electric-field-induced reversible ferroelastic strain effect, which can be enhanced by 84% under the magnetic field. Moreover, the magnetoresistance can be effectively tuned by the electrically driven ferroelastic strain. These findings reveal that the ferroelastic strain and the magnetic field strongly correlate with each other and are mediated by phase separation. Our work provides an approach to design strain-engineered multifunctional memory devices based on complex oxides by introducing an extra magnetic field stimulus. *Published by AIP Publishing*. https://doi.org/10.1063/1.5013924

The past few decades have witnessed fascinating discoveries in complex oxides, which are typified by the emergence of high temperature superconductivity,[1] colossal magnetoresistance (MR),[2] metal-insulator transition,[3] charge ordering (CO)/orbital ordering,[4] and electronic phase separation.[5] Half-doped $Nd_{0.5}Sr_{0.5}MnO_3$ (NSMO) locates at the phase boundary between the ferromagnetic (FM) metallic phase and the charge-ordering antiferromagnetic insulating phase,[6] which is sensitive to various external stimuli including magnetic field, electric field, current, strain, and light,[7–12] due to strong coupling among the lattice, spin, charge, and orbital degrees of freedom. The subtle balance of free energy between the coexisting FM and CO phases can be easily tipped by these external stimuli, resulting in drastic modification of phase separation and physical properties. For example, Kuwahara *et al.*[7] reported that the CO phase can be completely melted into the FM phase under the magnetic field above 7 T with the resistance reduction by three orders of magnitude in NSMO crystals. Moreover, Nakamura *et al.*[10] observed that in-plane anisotropic strain favors a clear first-order CO phase transition in NSMO(011) films, while Prellier *et al.*[11] found strain relaxation-induced phase transition from the CO to the FM state with the increasing thickness from 20 to 200 nm in NSMO(001) films, giving rise to the shift of metal-insulator transition temperature from $T_{MI} = 200$ to 240 K. However, using this static strain control method, one cannot rule out the impacts of other factors (e.g., oxygen content, defects, disorder, and dead layer) on the CO phase and magnetic and electronic properties. Fortunately, ferroelectric $Pb(Mg_{1/3}Nb_{2/3})O_3$-$PbTiO_3$ (PMN-PT) single crystals have been recently used as piezoelectrically active substrates to grow a variety of functional oxide thin films, such as colossal magnetoresistive manganites,[13] high temperature superconductors,[14] and multiferroic bismuth ferrites,[15] so that the lattice strain and physical properties of these thin films can be *in situ* dynamically manipulated by simply applying an electric field to the PMN-PT. Further, the electrically driven nonvolatile switching of lattice-coupled physical parameters has been achieved in $Co_{40}Fe_{40}B_{20}$/PMN-PT(001),[16] $Fe_{60}Co_{20}B_{20}$/PMN-PT(011),[17] Fe_3O_4/PMN-PT(011),[18] VO_2/PMN-PT(111),[19] and $SrRuO_3$/PMN-PT(111)[20] systems through non-linear lattice strain effects arising from non-180° ferroelastic domain switching, which is indispensable from a device application point of view. Despite the efforts devoted to the modulation of physical properties of the NSMO films using either the magnetic field or lattice strain, *in situ* multi-field tuning of the CO phase and the resultant functionalities is still very limited. There is no doubt that a systematic investigation of combined lattice strain and magnetic field control of phase separation and related order parameters would help to elucidate the straintronics physics and coupling effect of lattice strain and magnetic field in perovskite manganites, which is also important to design energy-efficient multifunctional storage devices by exploiting an additional spin degree of freedom.

In this work, we grew charge-ordered NSMO thin films on ferroelectric PMN-PT(011) single-crystal substrates and realized nonvolatile resistance tuning of the NSMO films at room temperature using the electric-field-induced reversible non-180° ferroelastic domain switching of the PMN-PT. The CO state of the films can be robustly modified by both the

a)Author to whom correspondence should be addressed: zhengm@mail.ustc.edu.cn

ferroelastic strain and magnetic field, leading to the change of phase separation tendency associated with adjustable magnetoresistance and strain effects. We also paid particular attention to the mutual interaction between the ferroelastic strain and the magnetic field, and the design of electrically tunable multifunctional nonvolatile memory devices by adding the magnetic field as an extra control parameter.

NSMO films (38 nm thick) were fabricated on one-side-polished PMN-PT(011) single-crystal substrates using pulsed laser deposition. The film thickness was chosen in order to obtain a stronger electric-field-induced strain effect but avoid the stronger strain inhomogeneity expected in thicker films and the interfacial charge effect in ultrathin films. The crystal structure and epitaxial properties of the films were analyzed using a high resolution Bruker D8 Discover X-ray diffractometer (XRD) attached with a 4-bounce Ge(220) monochromator and Cu $K_{\alpha 1}$ radiation ($\lambda = 1.5406$ Å). The magnetotransport properties of the films were measured using the standard four-probe method on a physical property measurement system (PPMS-9, Quantum Design) with the magnetic field applied parallel to the sample plane. A Keithley 6487 voltage source was employed to apply electric fields to the PMN-PT substrate through the conducting NSMO film and the bottom silver electrode. Figures 1(a) and 1(b) depict the schematic of the experimental setups for *in situ* measurements of resistance and out-of-plane strain of the NSMO/PMN-PT structure, respectively. Prior to the measurements, a large dc electric field of $E = +8$ kV/cm across the structure was applied for 30 min to ensure that the PMN-PT substrate is fully positively polarized.

Figure 1(c) shows the XRD θ–2θ scan pattern for the NSMO/PMN-PT structure. The NSMO film is highly (011)-oriented and of single phase. XRD ϕ-scans taken on the NSMO(111) and PMN-PT(111) reflections yield two sets of twofold symmetrical diffraction peaks [see Fig. 1(d)], implying a "cube-on-cube" heteroepitaxy nature. The schematic diagram of the in-plane lattice arrangements for the orthorhombic NSMO unit cell on the PMN-PT substrate is shown in the inset of Fig. 1(c). The initial strain state of the NSMO film can be determined by analyzing its main peak in the XRD scan curve. The out-of-plane lattice spacing d_{011} of the NSMO film (~2.705 Å) is smaller than that of the bulk value (~2.719 Å),[21] which indicates that the NSMO film is subject to an out-of-plane compressive strain (−0.51%) accompanied by an effective in-plane tensile strain. Based on the Poisson relation $\delta\varepsilon_{zz} = -2\nu/(1-\nu)\delta\varepsilon_{xx}$[22] and Poisson's ratio $\nu = 0.49$,[10] the in-plane tensile strain of the NSMO film can be estimated to be 0.27%. This result corresponds to the smaller lattice parameters of the NSMO bulk ($a \sim b \sim c \sim 3.845$ Å)[21] compared with those of the PMN-PT substrate ($a \sim b \sim c \sim 4.02$ Å).

Figure 2(a) illustrates *in situ* electric field manipulation of the resistance of the NSMO film under both bipolar and unipolar voltage cycling at room temperature. Upon cycling a large bipolar electric field with an amplitude of $E = 8$ kV/cm, a butterfly-like curve of the resistance versus electric field was observed, which is consistent with the typical butterfly-like curve of the in-plane strain versus electric field expected for the PMN-PT substrate.[17] This finding reveals that the resistance change in the NSMO film is induced by the electric-field-induced lattice strain in the PMN-PT substrate. In contrast, when cycling a small unipolar electric field [e.g., $E = 3$ kV/cm $< E_{C(PMN-PT)}$], a hysteresis-like loop of $\Delta R/R$ to E was displayed (peak curve). Here, $\Delta R/R$ is defined as $\Delta R/R = [R(E) - R(P_r^+)]/R(P_r^+)$. The resistance change process can be ascribed to the stable and reversible ferroelastic domain switching in the PMN-PT substrate.[16–20] In the rhombohedral PMN-PT crystal, the polarization vectors align along eight body diagonal directions of the pseudocubic unit cell with four structural domains (r1, r2, r3, and r4). Upon applying a large positive $E = +8$ kV/cm prior to the measurement, the PMN-PT will be fully positively poled (denoted by P_r^+) with the polarization pointing to r1$^-$ and r2$^-$ (i.e., the

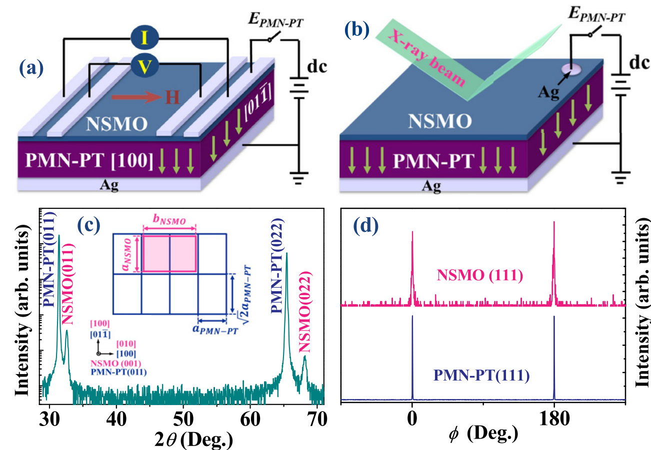

FIG. 1. Schematic of the experimental setups for *in situ* measurements of (a) resistance and (b) out-of-plane strain of the NSMO/PMN-PT structure, respectively. (c) XRD θ-2θ scan pattern of the NSMO/PMN-PT structure. The inset shows a schematic of in-plane lattice arrangements for the orthorhombic NSMO unit cell on the PMN-PT(011) substrate. (d) XRD ϕ scans taken on the NSMO(111) and PMN-PT(111) diffraction peaks.

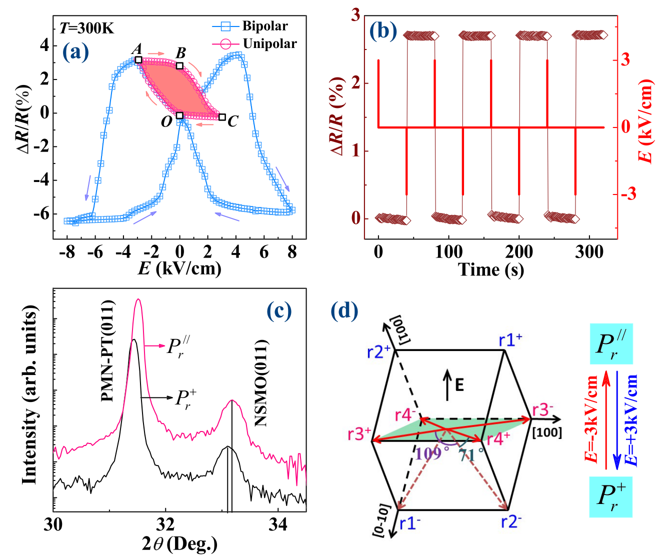

FIG. 2. (a) Electric-field-induced relative resistance variation $\Delta R/R$ of the NSMO film as a function of bipolar and unipolar E applied to the PMN-PT at $T = 300$ K. (b) Nonvolatile resistance tuning of the NSMO film by a sequence of pulse electric fields at $T = 300$ K. (c) XRD θ-2θ scan patterns for the PMN-PT(011) substrate and the NSMO(011) film under the P_r^+ and $P_r^{//}$ states, respectively. (d) Schematic of the polarization vectors in the rhombohedral phase from the P_r^+ to the $P_r^{//}$ state for the PMN-PT(011).

[0-1-1] direction) [marked by dashed arrows in Fig. 2(d)]. Then, after applying a small negative $E = -3$ kV/cm, the PMN-PT will be partially depolarized. The polarization switching pathways include 109° ferroelastic switching (e.g., from r2$^-$ to r3$^+$) and 71° ferroelastic switching (e.g., from r2$^-$ to r4$^+$), leading to the polarization vectors rotated from the downward to the in-plane direction (denoted by $P_r^{//}$). This domain switching can produce an in-plane tensile strain in the PMN-PT substrate and the NSMO film, as reflected by the diffraction peak shift to higher Bragg angles in Fig. 2(c). We calculated the reduced out-of-plane compressive strain in the NSMO film as 0.296%. Using the Poisson relation, the enhanced in-plane tensile strain is estimated to be 0.154%. Consequently, the film resistance evolves from ***O*** to ***A*** and then to the ***B*** state ($\Delta R/R \sim 2.7\%$). Afterwards, with the application and removal of another small positive $E = +3$ kV/cm, the resistance can recover to the initial ***O*** state due to the release of the previously induced remnant in-plane tensile strain. These two stable and switchable resistance states (***O*** and ***B*** states) can be achieved by reversing the applied electric field near the coercive field to dynamically rotate the polarization between the downward and in-plane directions (P_r^+ and $P_r^{//}$ states) in the PMN-PT substrate. On the basis of such an electrically driven ferroelastic strain effect, we demonstrated a rudimental manifestation of the applicability of an energy-efficient information storage element. As depicted in Fig. 2(b), the nonvolatile logic states were written by applying electric field pulses with the amplitude of $E = +3.0$ kV/cm for the "OFF" state and $E = -3.0$ kV/cm for the "ON" state, respectively. The domain-engineered ferroelastic switching presents a potential strategy for designing energy-efficient nonvolatile memory devices.

Figure 3(a) shows the temperature dependence of the resistance at several magnetic fields for the NSMO film under both the out-of-plane (P_r^+) and in-plane ($P_r^{//}$) polarization states of the PMN-PT, respectively. For the P_r^+ state and $H = 0$ T, the resistance increases upon cooling and undergoes a charge-ordering phase transition at $T_{CO} \sim 226$ K. Here, T_{CO} can be derived from the $d(\ln R)/d(T^{-1}) - T$ curve[23] shown in the inset of Fig. 3(a). Associated with the polarization switching from the P_r^+ to the $P_r^{//}$ state, a dramatic increase in the resistance and T_{CO} [see inset of Fig. 3(b)] was found with or without the application of an external magnetic field, hinting that the FM metallic phase was largely converted into the CO insulating phase due to the in-plane tensile strain-induced enhancement of the electron-lattice coupling and suppression of the double exchange interaction.[24] As shown in the inset of Fig. 3(b), all the values of T_{CO} were calculated by recording the peak number in the $d(\ln R)/d(T^{-1}) - T$ curve in the inset of Fig. 3(a). It is noteworthy that similar to that reported in the $LaMnO_{3+\delta}$ and $La_{0.875}Sr_{0.125}MnO_3$ systems,[25–27] T_{CO} rises with the magnetic field regardless of whether for the P_r^+ or $P_r^{//}$ state [see inset of Fig. 3(b)], which is caused by the reduction in the Jahn-Teller distortion and the corresponding energy gain in the FM metallic phase.[27] The similarity in the responses of the magnetic field to T_{CO} observed in the NSMO film and the charge-ordered $LaMnO_{3+\delta}$ ($La_{0.875}Sr_{0.125}MnO_3$) system provides an collateral evidence that the upturn of the resistance near $T = 226$ K ($T = 230$ K) for the P_r^+ ($P_r^{//}$) state

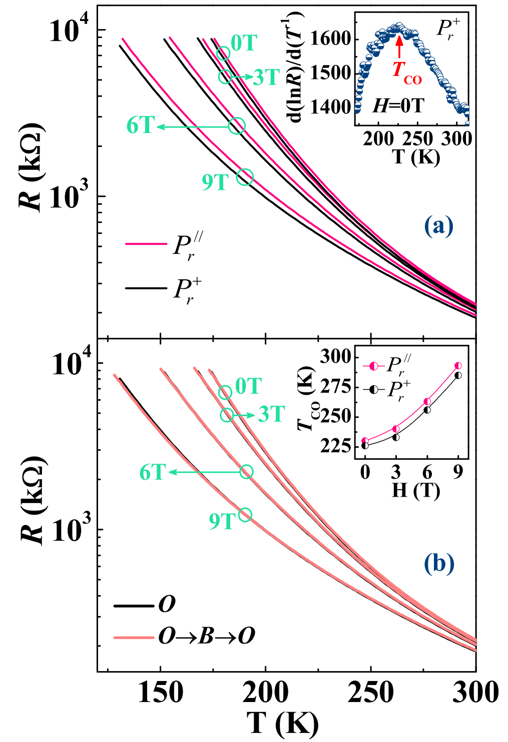

FIG. 3. (a) Temperature dependence of the resistance for the NSMO film under magnetic fields as stated when the PMN-PT substrate was in the P_r^+ and $P_r^{//}$ states, respectively. The inset shows the $d(\ln R)/d(T^{-1}) - T$ curve. (b) Resistance curves for two consecutive P_r^+ states (***O*** and ***O***→***B***→***O***). The inset shows T_{CO} versus H curves for the P_r^+ and $P_r^{//}$ states, respectively.

indeed stems from the charge-/orbital-ordering phase transition. Moreover, as shown in Fig. 3(b), whether the NSMO film was at $H = 0$, 3, 6, or 9 T, the resistance curves for the P_r^+ state (***O***) have similar patterns to those of the next consecutive P_r^+ state after a cycle (***O***→***B***→***O***), disclosing electrically stable and reversible ferroelastic strain effect of the NSMO/PMN-PT structure.

To unveil the coupling effect of the ferroelastic strain and magnetic field, we recorded the electroresistance (*ER*) against temperature for the NSMO/PMN-PT structure in Fig. 4(a). Here, the *ER*, $ER = [R(P_r^{//}) - R(P_r^+)]/R(P_r^+)$, is the ferroelastic-strain tunability of resistance. For $H = 0$ T, the *ER* increases monotonously on cooling and reaches a maximal value of 7.8% at $T = 174$ K, suggesting increased sensitivity of the CO phase to the lattice strain at low temperatures. More importantly, the *ER* is dramatically reinforced under the external magnetic field especially at low temperatures. For example, *ER* at $T = 180$ K increases from 7.5% for $H = 0$ T to 13.8% for $H = 9$ T, an enhancement of 84% [see inset of Fig. 4(a)]. In the low temperature region, the CO insulating phase dominates over the FM metallic phase in the NSMO film. The application of the magnetic field would convert a large fraction of the CO phase to the FM phase and thus enhances the phase separation tendency, thereby bringing a stronger ferroelastic strain effect of the NSMO/PMN-PT structure.[24] The mutual correlation between the magnetic field and the ferroelastic strain is manifested not only by the magnetically tunable electroresistance effect (i.e., ferroelastic strain effect) but also by the strain tunable magnetoresistance effect. The latter is shown in Fig. 4(b),

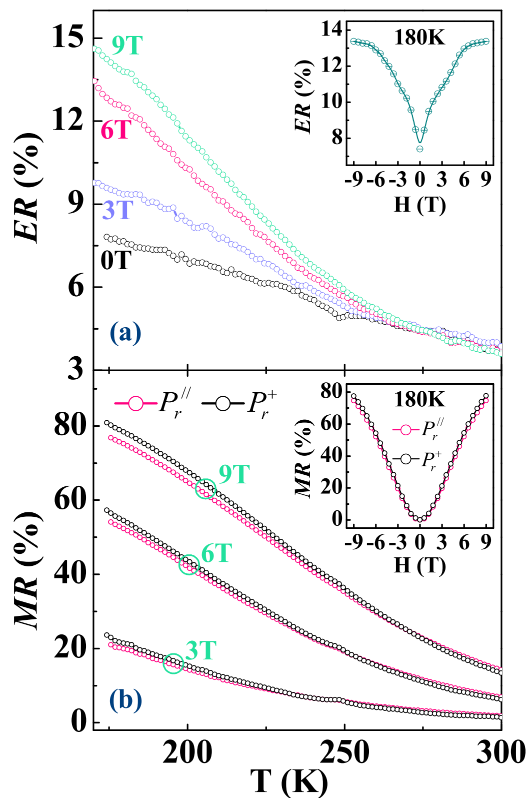

FIG. 4. (a) Temperature dependence of electroresistance (*ER*) for the NSMO film under magnetic fields as stated. The inset shows *ER* versus *H* curve at $T = 180$ K. (b) Temperature dependence of magnetoresistance (*MR*) for the NSMO film under the P_r^+ and $P_r^{//}$ states, respectively. The inset shows corresponding *MR* versus *H* curves at $T = 180$ K.

where the *MR* of the NSMO film was measured under the P_r^+ and $P_r^{//}$ states, respectively. Here, *MR* is defined as $MR = [R(0) - R(H)]/R(0)$. Upon the polarization being rotated from the P_r^+ to the $P_r^{//}$ state, the *MR* is reduced particularly at low temperatures, which is better seen in the inset of Fig. 4(b). For example, the relative change in *MR*, $\Delta MR/MR = [MR(P_r^+) - MR(P_r^{//})]/MR(P_r^+)$, reaches 7.2% at $T = 180$ K for $H = 3$ T. The electrically controlled magnetoresistance effect can be attributed to the ferroelastic (in-plane tensile) strain-induced enhancement of the CO phase, which suppresses the phase separation tendency and weakens the magnetic field effect on the NSMO/PMN-PT structure. All these data explicitly demonstrate that the ferroelastic strain strongly couples with the magnetic field, which is essentially mediated by the strength of phase separation. We note that the *ER* (or *MR*) responses sharply to the magnetic field (or ferroelastic strain) at low temperatures, while remains almost unchanged at high temperatures. This means that the CO phase in the present NSMO film is more sensitive to the magnetic field (or ferroelastic strain) effect than other charge/orbital disorder phases,[27,28] such as paramagnetic insulating phase, which also proves the effectiveness of magnetically and ferroelastically tunable phase separation.

In summary, we have reported the ferroelastic strain and magnetic field co-control of phase separation driven functionalities using a simple NSMO/PMN-PT multiferroic heterostructure. The bistable and nonvolatile resistance states can be *in situ* reversibly switched by applying appropriate pulse electric fields, which is closely related to the electric-field-induced 109° and 71° ferroelastic domain switching and induced intermediate in-plane strain state. Such a ferroelastic strain effect can be magnetically reinforced by 84%. Moreover, a visible reduction in the magnetoresistance was observed by the electric-field-induced ferroelastic strain at low temperatures. These results establish strong coupling between the magnetic field and the ferroelastic strain, which can be plausibly explained in terms of the phase separation model. Our findings provide a framework for realizing multi-field modulation of phase separation in complex oxides, which allows for the integration of an additional functionality (e.g., magnetic sensor) in the energy-efficient nonvolatile storage devices.

This work was supported by the National Key Project for Basic Research (Grant No. 2014CB921002), the National Natural Science Foundation of China (Grant Nos. 11374225, 11574227, 51572280, and 11504432), the Foundation of the Shanghai Committee for Science and Technology (Grant No. 15JC1403600), the Fundamental Research Funds for the Central Universities (Grant No. 18CX02046A), the Research Grant Council of Hong Kong (Project Nos. HKU 702112P and HKU 701813), and the Qingdao Science and Technology Program for Youth (Grant No. 16-5-1-6-jch).

[1]P. A. Lee, N. Nagaosa, and X.-G. Wen, Rev. Mod. Phys. **78**, 17 (2006).
[2]M. Uehara, S. Mori, C. H. Chen, and S.-W. Cheong, Nature **399**, 560 (1999).
[3]N. Takubo, I. Onishi, K. Takubo, T. Mizokawa, and K. Miyano, Phys. Rev. Lett. **101**, 177403 (2008).
[4]R. Schmidt, Phys. Rev. B **77**, 205101 (2008).
[5]A. Biswas, M. Rajeswari, R. C. Srivastava, T. Venkatesan, R. L. Greene, Q. Lu, A. L. de Lozanne, and A. J. Millis, Phys. Rev. B **63**, 184424 (2001).
[6]Y. Tokura, Rep. Prog. Phys. **69**, 797 (2006).
[7]H. Kuwahara, Y. Tomioka, A. Asamitsu, Y. Moritomo, and Y. Tokura, Science **270**, 961 (1995).
[8]L. P. Chen, F. Wang, Y. S. Chen, Y. Sun, and J. Gao, Europhys. Lett. **100**, 47006 (2012).
[9]J. Gao, S. Q. Shen, T. K. Li, and J. R. Sun, Appl. Phys. Lett. **82**, 4732 (2003).
[10]M. Nakamura, Y. Ogimoto, H. Tamaru, M. Izumi, and K. Miyano, Appl. Phys. Lett. **86**, 182504 (2005).
[11]W. Prellier, A. Biswas, M. Rajeswari, T. Venkatesan, and R. L. Greene, Appl. Phys. Lett. **75**, 397 (1999).
[12]K. Miyasaka, M. Nakamura, Y. Ogimoto, H. Tamaru, and K. Miyano, Phys. Rev. B **74**, 012401 (2006).
[13]C. Thiele, K. Dörr, O. Bilani, J. Rödel, and L. Schultz, Phys. Rev. B **75**, 054408 (2007).
[14]S. Trommler, R. Hühne, K. Iida, P. Pahlke, S. Haindl, L. Schultz, and B. Holzapfel, New J. Phys. **12**, 103030 (2010).
[15]M. D. Biegalski, D. H. Kim, S. Choudhury, L. Q. Chen, H. M. Christen, and K. Dörr, Appl. Phys. Lett. **98**, 142902 (2011).
[16]S. Zhang, Y. G. Zhao, P. S. Li, J. J. Yang, S. Rizwan, J. X. Zhang, J. Seidel, T. L. Qu, Y. J. Yang, Z. L. Luo *et al.*, Phys. Rev. Lett. **108**, 137203 (2012).
[17]M. Liu, B. M. Howe, L. Grazulis, K. Mahalingam, T. X. Nan, N. X. Sun, and G. J. Brown, Adv. Mater. **25**, 4886 (2013).
[18]M. Liu, J. Hoffman, J. Wang, J. X. Zhang, B. Nelson-Cheeseman, and A. Bhattacharya, Sci. Rep. **3**, 1876 (2013).
[19]B. W. Zhi, G. Y. Gao, H. R. Xu, F. Chen, X. L. Tan, P. F. Chen, L. F. Wang, and W. B. Wu, ACS Appl. Mater. Interfaces **6**, 4603 (2014).
[20]M. Zheng, H. Ni, Y. P. Qi, W. Y. Huang, J. L. Zeng, and J. Gao, Appl. Phys. Lett. **110**, 182403 (2017).
[21]Q. Qian, T. A. Tyson, C.-C. Kao, W. Prellier, J. Bai, A. Biswas, and R. L. Greene, Phys. Rev. B **63**, 224424 (2001).
[22]S. P. Timoshenko and J. N. Goodier, *Theory of Elasticity* (McGraw-Hill, New York, 1987), Chap. 2.

[23]A. P. Ramirez, P. Schiffer, S.-W. Cheong, C. H. Chen, W. Bao, T. T. M. Palstra, P. L. Gammel, D. J. Bishop, and B. Zegarski, Phys. Rev. Lett. **76**, 3188 (1996).
[24]Q. X. Zhu, M. Zheng, M. M. Yang, X. M. Li, Y. Wang, X. Shi, H. L. W. Chan, H. S. Luo, X. G. Li, and R. K. Zheng, Appl. Phys. Lett. **103**, 132910 (2013).
[25]R. K. Zheng, H.-U. Habermeier, H. L. W. Chan, C. L. Choy, and H. S. Luo, Phys. Rev. B **81**, 104427 (2010).
[26]S. Uhlenbruck, R. Teipen, R. Klingeler, B. Büchner, O. Friedt, M. Hücker, H. Kierspel, T. Niemöller, L. Pinsard, A. Revcolevschi, and R. Gross, Phys. Rev. Lett. **82**, 185 (1999).
[27]J. Wang, F. X. Hu, R. W. Li, J. R. Sun, and B. G. Shen, Appl. Phys. Lett. **96**, 052501 (2010).
[28]L. Chen, F. X. Hu, J. Wang, J. Shen, J. R. Sun, B. G. Shen, J. H. Yin, and L. Q. Pan, J. Appl. Phys. **109**, 07D713 (2011).